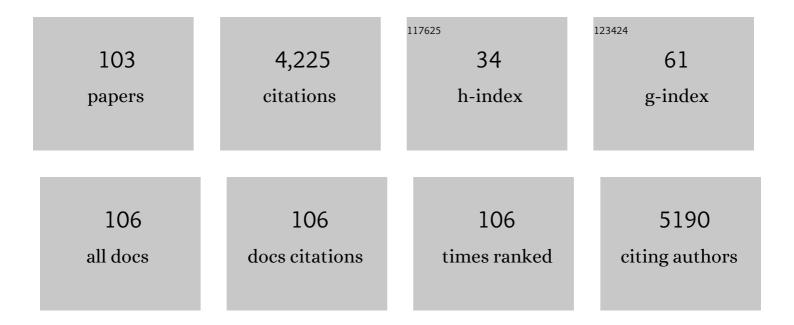
Yeon-Tae Yu

List of Publications by Year in descending order

Source: https://exaly.com/author-pdf/1475/publications.pdf Version: 2024-02-01



#	Article	IF	CITATIONS
1	The role of gold catalyst on the sensing behavior of ZnO nanorods for CO and NO2 gases. Sensors and Actuators B: Chemical, 2012, 165, 133-142.	7.8	245
2	Synthesis of Coreâ^'Shell Au@TiO ₂ Nanoparticles with Truncated Wedge-Shaped Morphology and Their Photocatalytic Properties. Langmuir, 2009, 25, 6438-6447.	3.5	226
3	Noble metal@metal oxide semiconductor core@shell nano-architectures as a new platform for gas sensor applications. RSC Advances, 2015, 5, 76229-76248.	3.6	185
4	Solvothermal Synthesis of ZnO Nanostructures and Their Morphology-Dependent Gas-Sensing Properties. ACS Applied Materials & amp; Interfaces, 2013, 5, 3026-3032.	8.0	183
5	Facile Approach to Synthesize Au@ZnO Core–Shell Nanoparticles and Their Application for Highly Sensitive and Selective Gas Sensors. ACS Applied Materials & Interfaces, 2015, 7, 9462-9468.	8.0	167
6	Au@NiO core-shell nanoparticles as a p-type gas sensor: Novel synthesis, characterization, and their gas sensing properties with sensing mechanism. Sensors and Actuators B: Chemical, 2018, 268, 223-231.	7.8	162
7	Au@Cu ₂ O core–shell nanoparticles as chemiresistors for gas sensor applications: effect of potential barrier modulation on the sensing performance. Nanoscale, 2014, 6, 581-588.	5.6	150
8	Synthesis of flower-like ZnO microstructures for gas sensor applications. Sensors and Actuators B: Chemical, 2013, 178, 107-112.	7.8	143
9	Citrate-assisted hydrothermal synthesis of single crystalline ZnO nanoparticles for gas sensor application. Sensors and Actuators B: Chemical, 2012, 173, 58-65.	7.8	133
10	Microwave assisted hydrothermal synthesis of single crystalline ZnO nanorods for gas sensor application. Materials Letters, 2012, 68, 90-93.	2.6	107
11	Glucose-assisted synthesis of Cu2O shuriken-like nanostructures and their application as nonenzymatic glucose biosensors. Sensors and Actuators B: Chemical, 2014, 203, 471-476.	7.8	98
12	Fabrication of aggregated In2O3 nanospheres for highly sensitive acetaldehyde gas sensors. Journal of Alloys and Compounds, 2019, 772, 834-842.	5.5	90
13	Examination of Au/SnO2 core-shell architecture nanoparticle for low temperature gas sensing applications. Sensors and Actuators B: Chemical, 2011, 157, 444-449.	7.8	84
14	Superfast and efficient hydrogen gas sensor using PdAu _{alloy} @ZnO core–shell nanoparticles. Journal of Materials Chemistry A, 2020, 8, 12968-12974.	10.3	81
15	Enhanced H ₂ gas sensing properties of Au@In ₂ O ₃ core–shell hybrid metal–semiconductor heteronanostructures. CrystEngComm, 2016, 18, 3655-3666.	2.6	78
16	Effect of Au Nanorods on Potential Barrier Modulation in Morphologically Controlled Au@Cu ₂ O Core–Shell Nanoreactors for Gas Sensor Applications. ACS Applied Materials & Interfaces, 2014, 6, 7491-7497.	8.0	75
17	Hydrothermal synthesis of single-crystalline nanocubes of Co3O4. Materials Letters, 2008, 62, 1006-1009.	2.6	63
18	Hydrothermal synthesis of In2O3 nanocubes for highly responsive and selective ethanol gas sensing. Journal of Alloys and Compounds, 2020, 820, 153133.	5.5	59

#	Article	IF	CITATIONS
19	Construction of novel hybrid PdO–ZnO p–n heterojunction nanostructures as a high-response sensor for acetaldehyde gas. CrystEngComm, 2019, 21, 5084-5094.	2.6	57
20	Microwave assisted hydrothermal synthesis of Au@TiO2 core–shell nanoparticles for high temperature CO sensing applications. Sensors and Actuators B: Chemical, 2013, 186, 633-639.	7.8	54
21	Functionalization of ZnO nanorods by CuO nanospikes for gas sensor applications. RSC Advances, 2014, 4, 23604.	3.6	53
22	Au@CeO2 nanoparticles supported Pt/C electrocatalyst to improve the removal of CO in methanol oxidation reaction. Journal of Catalysis, 2019, 377, 589-599.	6.2	52
23	Fabrication of flower-like ZnO microstructures from ZnO nanorods and their photoluminescence properties. Materials Chemistry and Physics, 2010, 124, 406-412.	4.0	49
24	Synthesis of plasmonic Ag@SnO ₂ core–shell nanoreactors for xylene detection. RSC Advances, 2015, 5, 17653-17659.	3.6	46
25	Synthesis of TiO ₂ hollow spheres by selective etching of Au@TiO ₂ core–shell nanoparticles for dye sensitized solar cell applications. RSC Advances, 2014, 4, 3529-3535.	3.6	45
26	Pt-loaded Au@CeO ₂ core–shell nanocatalysts for improving methanol oxidation reaction activity. Journal of Materials Chemistry A, 2019, 7, 26996-27006.	10.3	45
27	Plasmonically driven photocatalytic hydrogen evolution activity of a Pt-functionalized Au@CeO ₂ core–shell catalyst under visible light. Journal of Materials Chemistry A, 2020, 8, 7687-7694.	10.3	45
28	Fabrication and properties of flower-shaped Pt@TiO2 core–shell nanoparticles. Materials Letters, 2010, 64, 2208-2210.	2.6	44
29	Synthesis of floral assembly with single crystalline ZnO nanorods and its CO sensing property. Sensors and Actuators B: Chemical, 2012, 161, 748-754.	7.8	44
30	Effect of core and surface area toward hydrogen gas sensing performance using Pd@ZnO core-shell nanoparticles. Journal of Colloid and Interface Science, 2021, 587, 252-259.	9.4	44
31	Insightful understanding of hot-carrier generation and transfer in plasmonic Au@CeO2 core–shell photocatalysts for light-driven hydrogen evolution improvement. Applied Catalysis B: Environmental, 2021, 286, 119947.	20.2	43
32	Preparation of nanocrystalline TiO2-coated coal fly ash and effect of iron oxides in coal fly ash on photocatalytic activity. Powder Technology, 2004, 146, 154-159.	4.2	40
33	Anisotropic Thermal Interface Materials: Directional Heat Transfer in Uniaxially Oriented Liquid Crystal Networks. ACS Applied Materials & Interfaces, 2018, 10, 35557-35562.	8.0	40
34	lonic liquid-assisted preparation of Ag-CeO2 nanocomposites and their improved photocatalytic activity. Materials and Design, 2018, 159, 186-194.	7.0	39
35	lonic liquid-supported synthesis of CeO2 nanoparticles and its enhanced ethanol gas sensing properties. Materials Chemistry and Physics, 2019, 231, 1-8.	4.0	35
36	Synthesis of Au/SnO2 core–shell structure nanoparticles by a microwave-assisted method and their optical properties. Journal of Solid State Chemistry, 2011, 184, 312-316.	2.9	34

#	Article	IF	CITATIONS
37	Remoteâ€Controllable Molecular Knob in the Mesomorphic Helical Superstructures. Advanced Functional Materials, 2016, 26, 4242-4251.	14.9	34
38	Synthesis and characterization of porous ZnO nanoparticles by hydrothermal treatment of as pure aqueous precursor. Materials Research Bulletin, 2011, 46, 525-530.	5.2	32
39	Synthesis, growth mechanism and photoluminescence of monodispersed cubic shape Ce doped YAG nanophosphor. Ceramics International, 2012, 38, 235-242.	4.8	32
40	Ultraviolet-C Photodetector Fabricated Using Si-Doped n-AlGaN Nanorods Grown by MOCVD. ACS Photonics, 2017, 4, 2595-2603.	6.6	32
41	Defect-rich N-doped CeO ₂ supported by N-doped graphene as a metal-free plasmonic hydrogen evolution photocatalyst. Journal of Materials Chemistry A, 2021, 9, 10217-10230.	10.3	32
42	Transparent, pressure-sensitive, and healable e-skin from a UV-cured polymer comprising dynamic urea bonds. Journal of Materials Chemistry A, 2019, 7, 3101-3111.	10.3	31
43	Gas sensing properties of single crystalline ZnO nanowires grown byÂthermal evaporation technique. Current Applied Physics, 2013, 13, 1769-1773.	2.4	30
44	Synthesis of Au/TiO2Core–Shell Nanoparticles from Titanium Isopropoxide and Thermal Resistance Effect of TiO2Shell. Japanese Journal of Applied Physics, 2007, 46, 2567-2570.	1.5	29
45	Synthesis of Au@SnO2 core–shell nanoparticles with controllable shell thickness and their CO sensing properties. Materials Chemistry and Physics, 2015, 166, 87-94.	4.0	28
46	Triple phase boundary and power density enhancement in PEMFCs of a Pt/C electrode with double catalyst layers. RSC Advances, 2019, 9, 15635-15641.	3.6	26
47	High response and selectivity toward hydrogen gas detection by In2O3 doped Pd@ZnO core-shell nanoparticles. Journal of Alloys and Compounds, 2021, 854, 157280.	5.5	26
48	Plasmonic Au nanoclusters dispersed in nitrogen-doped graphene as a robust photocatalyst for light-to-hydrogen conversion. Journal of Materials Chemistry A, 2021, 9, 22810-22819.	10.3	26
49	Synthesis and characterization of Au/TiO2 core-shell structure nanoparticles. Korean Journal of Chemical Engineering, 2003, 20, 1176-1182.	2.7	24
50	Ag@SnO2 core–shell structure nanocomposites. Chemical Physics Letters, 2007, 442, 101-104.	2.6	24
51	Synthesis of violet light emitting single crystalline ZnO nanorods by using CTAB-assisted hydrothermal method. Journal of Materials Science: Materials in Electronics, 2009, 20, 967-971.	2.2	24
52	Energy coupling processes in InGaN/GaN nanopillar light emitting diodes embedded with Ag and Ag/SiO2 nanoparticles. Journal of Materials Chemistry, 2012, 22, 21749.	6.7	24
53	Photopolymerization of Reactive Amphiphiles: Automatic and Robust Vertical Alignment Layers of Liquid Crystals with a Strong Surface Anchoring Energy. Macromolecules, 2016, 49, 23-29.	4.8	24
54	Superhigh sensing response and selectivity for hydrogen gas using PdPt@ZnO core-shell nanoparticles: Unique effect of alloyed ingredient from experimental and theoretical investigations. Sensors and Actuators B: Chemical, 2022, 354, 131083.	7.8	24

#	Article	IF	CITATIONS
55	Influence of carbon precursors on thermal plasma assisted synthesis of SiC nanoparticles. Advanced Powder Technology, 2014, 25, 640-646.	4.1	22
56	Stimuli-responsive liquid crystal physical gels based on the hierarchical superstructures of benzene-1,3,5-tricarboxamide macrogelators. Polymer Chemistry, 2017, 8, 1888-1894.	3.9	22
57	Synthesis and electrophoretic deposition of hollow-TiO2 nanoparticles for dye sensitized solar cell applications. Journal of Alloys and Compounds, 2016, 672, 212-222.	5.5	20
58	Polarized Light Emission from Uniaxially Oriented and Polymer-Stabilized AIE Luminogen Thin Films. Macromolecules, 2019, 52, 1739-1745.	4.8	20
59	Topochemical polymerization of dumbbell-shaped diacetylene monomers: relationship between chemical structure, molecular packing structure, and gelation property. Soft Matter, 2017, 13, 5759-5766.	2.7	19
60	CTAB-assisted hydrothermal synthesis of single-crystalline copper-doped ZnO nanorods and investigation of their photoluminescence properties. Journal of Materials Science: Materials in Electronics, 2010, 21, 1036-1041.	2.2	18
61	Revisiting the thickness reduction approach for near-foldable capacitive touch sensors based on a single layer of Ag nanowire-polymer composite structure. Composites Science and Technology, 2018, 165, 58-65.	7.8	18
62	Highly Efficient Photoelectrochemical Water Splitting Using GaN-Nanowire Photoanode with Tungsten Sulfides. ACS Applied Materials & Interfaces, 2020, 12, 58028-58037.	8.0	18
63	Synthesis and fluorescence properties of pure and metal-doped spherical ZnS particles from EDTA–metal complexes. Journal of Physics and Chemistry of Solids, 2008, 69, 153-160.	4.0	17
64	Quantum efficiency control of InGaN/GaN multi-quantum-well structures using Ag/SiO2 core-shell nanoparticles. Applied Physics Letters, 2011, 99, 251114.	3.3	17
65	Enhanced electrocatalytic property of Pt/C electrode with double catalyst layers for PEMFC. International Journal of Hydrogen Energy, 2019, 44, 24580-24590.	7.1	17
66	Light-to-Hydrogen Improvement Based on Three-Factored Au@CeO ₂ /Gr Hierarchical Photocatalysts. ACS Nano, 2022, 16, 7848-7860.	14.6	16
67	Synthesis of Nanosized Silicon Carbide Through Non-Transferred Arc Thermal Plasma. Plasma Chemistry and Plasma Processing, 2012, 32, 211-218.	2.4	15
68	Microwave assisted synthesis of flower-like ZnO and effect of annealing atmosphere on its photoluminescence property. Journal of Materials Science: Materials in Electronics, 2012, 23, 344-348.	2.2	15
69	Effect of the Nafion content in the MPL on the catalytic activity of the Pt/C-Nafion electrode prepared by pulsed electrophoresis deposition. International Journal of Hydrogen Energy, 2017, 42, 1181-1188.	7.1	15
70	Polyol-assisted synthesis of TiO2 nanoparticles in a semi-aqueous solvent. Journal of Physics and Chemistry of Solids, 2009, 70, 147-152.	4.0	14
71	Effect of the deposition time on the electrocatalytic activity of Pt/C catalyst electrodes prepared by pulsed electrophoresis deposition method. International Journal of Hydrogen Energy, 2013, 38, 3606-3613.	7.1	14
72	Hydrothermal growth and characterization of ZnO thin film on sapphire (0001) substrate with p-GaN buffer layer. Thin Solid Films, 2008, 516, 8244-8247.	1.8	13

#	Article	IF	CITATIONS
73	Conversion of ZnO microrods into microdisks like structures and its effect on photoluminescence properties. Ceramics International, 2013, 39, 8287-8291.	4.8	13
74	Preparation of Pt/C electrode with double catalyst layers by electrophoresis deposition method for PEMFC. International Journal of Hydrogen Energy, 2014, 39, 3381-3386.	7.1	13
75	Morphology controlled Ag@SiO2 core–shell nanoparticles by ascorbic acid reduction. Journal of Materials Science: Materials in Electronics, 2014, 25, 1156-1161.	2.2	13
76	Thermal plasma synthesis of Si/SiC nanoparticles from silicon and activated carbon powders. Ceramics International, 2016, 42, 16469-16473.	4.8	13
77	Fabrication and Characterization of a Capacitive Photodetector Comprising a ZnS/Cu Particle/Poly(vinyl butyral) Composite. ACS Applied Materials & Interfaces, 2019, 11, 4416-4424.	8.0	13
78	Core and dopant effects toward hydrogen gas sensing activity using Pd@N-CeO2 core–shell nanoflatforms. Journal of Industrial and Engineering Chemistry, 2021, 95, 325-332.	5.8	13
79			

#	Article	IF	CITATIONS
91	Synthesis and Photocatalytic Property of Metal@SnO2 Core–Shell Structure Nanocomposites. Journal of Nanoscience and Nanotechnology, 2011, 11, 453-457.	0.9	8
92	Improvement in the photoelectrochemical water-splitting performance using GaN nanowires with bundle structures. Journal of Materials Chemistry C, 2021, 9, 12802-12810.	5.5	8
93	Drastic improvement in photoelectrochemical water splitting performance over prolonged reaction time using new carrier-guiding semiconductor nanostructures. Journal of Materials Chemistry A, 2022, 10, 9821-9829.	10.3	8
94	Growth of ZnO thin film on p-GaN/sapphire (0001) by simple hydrothermal technique. Journal of Crystal Growth, 2008, 310, 570-574.	1.5	7
95	Sintering Behavior of Spark Plasma Sintered SiC with Si-SiC Composite Nanoparticles Prepared by Thermal DC Plasma Process. Nanoscale Research Letters, 2017, 12, 606.	5.7	7
96	Photoelectrochemical water-splitting using GaN pyramidal dots and their long-term stability in the two-electrode configuration. Journal of Materials Chemistry A, 2022, 10, 10355-10362.	10.3	7
97	Nano-architecture platinum catalyst layer prepared by electrophoresis deposition for PEM fuel cells. Journal of Solid State Electrochemistry, 2012, 16, 1377-1381.	2.5	6
98	Hydrothermal growth of single crystal ZnO nanorods on surface-modified graphite. Electronic Materials Letters, 2013, 9, 715-718.	2.2	6
99	Facile preparation of ZnO nanosheets and its photocatalytic activity in the degradation of rhodamine B dye under UV irradiation. Electronic Materials Letters, 2016, 12, 784-788.	2.2	6
100	Investigating the mechanism of uniform Ag@SiO2 core-shell nanostructures synthesis by a one-pot sol–gel method. Journal of Sol-Gel Science and Technology, 2020, 96, 679-689.	2.4	5
101	CO gas-sensing properties of CuO-TiN and CuO-TiN-TiO2 prepared by controlled oxidation of Cu-TiN composites. Metals and Materials International, 2015, 21, 330-336.	3.4	4
102	Pd supported N-doped CeO ₂ as an efficient hydrogen oxidation reaction catalyst in PEMFC. New Journal of Chemistry, 2020, 44, 17203-17207.	2.8	3
103	Electrophoretic deposition of CdSe@CdZnS–ZnS multi core–shell QDs for quantum efficiency control of InGaN/GaN MQW LEDs. RSC Advances, 2016, 6, 95032-95037.	3.6	1